AIP Journal of Applied Physics

Effects of activation by proton irradiation on silicon particle detector electric characteristics

S. Väyrynen, J. Räisänen, P. Tikkanen, I. Kassamakov, and E. Tuominen

Citation: Journal of Applied Physics **106**, 024908 (2009); doi: 10.1063/1.3168436
View online: http://dx.doi.org/10.1063/1.3168436
View Table of Contents: http://scitation.aip.org/content/aip/journal/jap/106/2?ver=pdfcov
Published by the AIP Publishing

Effects of activation by proton irradiation on silicon particle detector electric characteristics

S. Väyrynen,[1,a)] J. Räisänen,[1] P. Tikkanen,[1] I. Kassamakov,[2] and E. Tuominen[3]
[1]*Department of Physics, University of Helsinki, P.O. Box 64, FI-00014 University of Helsinki, Finland*
[2]*Department of Micro and Nanosciences, Helsinki University of Technology, P.O. Box 3000, FI-02015 TKK, Finland*
[3]*Helsinki Institute of Physics, University of Helsinki, P.O. Box 64, FI-00014 University of Helsinki, Finland*

(Received 12 December 2008; accepted 9 June 2009; published online 22 July 2009)

After irradiation with 7 and 9 MeV protons, activation-induced effects were encountered in measurements of current-voltage (*IV*) and capacitance-voltage (*CV*) characteristics for Czochralski and float-zone grown silicon particle detectors prepared on printed circuit boards with copper electrodes. With the present detector construction, the $^{30}\mathrm{Si}(p,n)^{30}\mathrm{P}$ and $^{63}\mathrm{Cu}(p,n)^{63}\mathrm{Zn}$ reactions induce dominant interference in such measurements. The daughter nuclides are positron emitters with half-lives of 2.5 and 38.5 min, respectively, and the slowing down of the emitted positrons generates a significantly large concentration of electron-hole pairs in the detector volume increasing the leakage current level and decreasing the breakdown voltage. The observed time-dependent characteristics were verified by modeling the activation of the detector structure and the resulting leakage current. As a result, the electrical measurements cannot be performed immediately after irradiation due to silicon activation, and, generally, materials becoming easily activated should be avoided in the detector concept. © *2009 American Institute of Physics*. [DOI: 10.1063/1.3168436]

I. INTRODUCTION

Silicon particle detectors are widely used in several applications, e.g., space, aviation, and radiation detection. In the upgrade of the large Hadron collider at CERN, the innermost silicon detectors will receive a fluence of 10^{16} particles/cm^2, well beyond the operational limit of the present silicon detectors. To develop detectors with better radiation hardness, more tests are thus needed. Testing for displacement damage, e.g., in *pn*-junction charge coupled devices[1,2] and silicon detectors,[3] is often carried out using 10 MeV protons. At that energy, predictions for any proton environment can be made utilizing the nonionizing energy loss curve.[4]

When energetic particles hit the detectors they produce irreversible crystallographic defects in the detector bulk material. The impact of the defects is seen as charge-carrier trapping, increased leakage current, and changed depletion voltage. While some defects are mobile already at moderately low temperatures and the crystal recovers after the irradiation, also more stable defects are produced. Ensuring exclusion of the end-of-range defects, predominantly point defects are produced in silicon by MeV-proton irradiation.[5] For studying such defects via positron annihilation spectroscopy, a facility has been constructed employing the 5 MV tandem accelerator of the Department of Physics at University of Helsinki.[5] The facility allows also on-line studies of electrical characteristics of silicon particle detectors.

However, unexpected problems were encountered in the measurements of current-voltage (*IV*) and capacitance-voltage (*CV*) characteristics. Especially, the very sensitive *CV* measurements triggered the detailed studies aiming to find out the cause of those problems. The origin of the cause was traced to activation, e.g., of the silicon crystal during the proton bombardment. Studies related to material activation induced by energetic particle bombardment and its effect on the on-line *IV* and *CV* characterizations of Si detectors have not been previously carried out due to the lack of proper facilities. In literature, only one previous work dealing with irradiation-induced activation of 4*H*-SiC particle detectors may be found where long-lived radioactivity induced by 24 GeV protons is discussed.[6] Our motivation has been to find the conceptual limits for on-line electrical characterization of particle detectors by irradiating Czochralski (Cz) and float-zone (Fz) grown silicon particle detectors with 7 and 9 MeV protons and following the time evolution of the representative *IV* and *CV* curves.

II. EXPERIMENTAL ARRANGEMENTS

Naturally, the employed materials and the detailed construction of the detector setup play an important role in the activation process. The particle detectors used in our studies were fabricated from *n*-type, 300 μm thick Cz-Si (resistivity $\sim$1100 Ω cm) supplied by Okmetic Ltd. and *n*-type, 280 μm thick Fz-Si (resistivity $\sim$1200 Ω cm) manufactured by Wacker. The $p^+/n^-/n^+$-structure, aluminum electrodes (0.5 μm thick), and the surrounding guard rings were processed at the Microelectronics Center of Helsinki University of Technology. In the present studies the guard rings were short circuited to the front electrode. The full depletion voltage was about 300 V for the Cz-Si diodes and 260 V for the Fz-Si diodes. The leakage current at full depletion was less than 1 nA for all nonirradiated diodes at temperature below 260 K. The detectors were glued with a carbon-based tape on a printed circuit board pad having gold plated (100

a)Electronic mail: samuli.vayrynen@helsinki.fi.

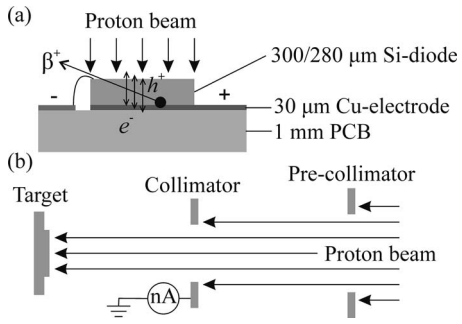

FIG. 1. (a) Cross-sectional view of the proton irradiated Si detectors. During their slowing down, the energetic positrons from the β-decay of the irradiation-induced radionuclides generate current inside the detector by creating electron-hole pairs. (b) Arrangement for the beam current monitoring.

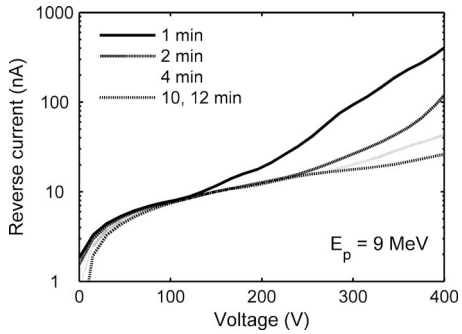

FIG. 2. Measured *IV* characteristics of a Cz detector at various times after 9 MeV proton irradiation to the fluence of 10^{14} cm^{-2}. The irradiation flux was about 1.7×10^{11} protons/cm^2 s and the detector temperature was kept constant at 220 K. Note that the curves of 10 and 12 min overlap.

nm thick) Cu electrodes (30 μm thick). The area of the Cz detectors was 8×8 mm^2 and of the Fz detectors 7×7 mm^2. The cross sectional layout of the detector structure is presented in Fig. 1(a).

The employed multipurpose cryogenic irradiation facility has been premiered in detail in Ref. 5, but since then it has been upgraded. The indirect beam current measurement based on a beam profilometer has been replaced with the setup illustrated in Fig. 1(b). The proton beam is swept over the precollimator (12×12 mm^2), and the beam current is measured just before the target from the main collimator having an aperture of 8.5×8.5 mm^2. The beam profilometer is used now only for beam homogeneity monitoring.

In the *IV* measurements the main component was a Keithley 2410 SourceMeter Unit (SMU), which was remotely controlled by a computer via a general purpose interface bus (GPIB) and using a LABVIEW-based code. The SMU and all cables are specified to withstand voltages up to 1 kV. The setup is also supplemented by a capacitance meter constructed at CERN especially developed for measurements of diodes with high leakage current. The capacitance meter combined with the SMU enables *CV* characterization up to 500 pF and 600 V with a resolution of one-tenth of a pF. A frequency of 18 kHz was used in the *CV* measurements.

III. MEASUREMENTS AND RESULTS

The detectors were bombarded with 6, 7, and 9 MeV protons to various fluences as listed in Table I. The irradiation fluxes varied from 4×10^{10} to 1.7×10^{11} protons/cm^2 s and the detector temperature was kept constant during the irradiations and measurements. Irradiations at several temperatures were carried out and the details of the various experimental parameters are provided in Table I. First *IV* curves were measured immediately (within $\sim$10 s) after the irradiation. As clear variation in the curve shapes was noted depending on the time when the measurement was started, the *IV* curves were measured repeatedly until the shape of the curve did not change. The measurement of a *IV* curve takes about 1 min. Typical measured *IV* characteristics of a Cz detector at various times after 9 MeV proton irradiation are presented in Fig. 2. The reverse current decreases systematically with time until it stabilizes in about 10 min. In Fig. 3 the *IV* characteristics are provided for a Cz detector irradiated with 7 MeV protons. The variation with time is not as prominent as in the case of the higher bombarding energy and the *IV* curve stabilizes in about 5 min.

Measured *CV* curves for Fz and Cz detectors at various times after irradiation with 9 MeV protons are presented in Fig. 4. The measurements were taken 10–25 min after the irradiation since in the *CV* measurements the signal cables could be connected to the sample only after the irradiation, and, therefore, a cooling time prior to measurements, in case of 9 MeV protons, was necessary to avoid personnel exposure to radiation. From Fig. 4 it may be concluded that the breakdown of the Fz detectors is clearly more abrupt than that of the Cz detectors. The estimated full depletion voltages of the Fz and Cz detectors are about 120 and 195 V, respectively. Importantly, similar detector recovery time dependence may be noted as in the *IV* measurements.

The recovery of the Fz-detector breakdown voltage after 9 MeV proton irradiation to fluences of 5×10^{11} and 5×10^{12} cm^{-2} is shown in Fig. 5. The data have been extracted from *CV* curves of diodes irradiated and measured at two different temperatures. According to Fig. 5, irradiation fluence has a strong influence on the breakdown voltage recovery but the effect of temperature is minor.

Based on the time-dependent features noted in Figs. 2–5 the role of material activation was suspected. To verify pos-

TABLE I. Experimental details of the silicon particle detector irradiations.

Material	No. of samples	Temperature ($\pm$1 K)	Proton energy (MeV)	Fluence (protons/cm^2)	Proton current (nA)
Cz-Si	7	220, 250	9	2×10^{11} to 10^{14}	20
Cz-Si	2	220	7	10^{13}–10^{14}	10
Cz-Si	4	230	6	10^{13} to 5×10^{13}	20
Fz-Si	4	220, 250	9	2×10^{11} to 10^{13}	5

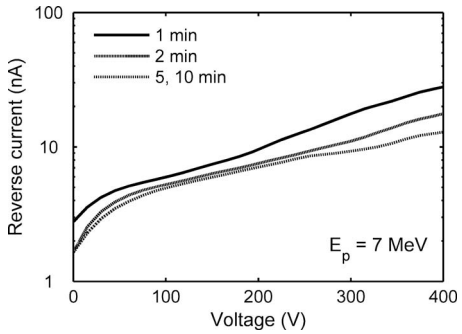

FIG. 3. As for Fig. 2, but after 7 MeV proton irradiation. The irradiation flux was about 2×10^{11} protons/cm^2 s. Note that the curves of 5 and 10 min overlap.

sible detector activation, gamma spectra of the irradiated detector structures were taken. In the measured γ-ray spectra strong peaks at 670 and 962 keV originating from β^+-decay of ^{63}Zn and the 511 keV annihilation peak were noted. The presence of ^{63}Zn is due to the 30 μm thick Cu electrode. It is evident that also silicon is activated and the relevant isotope leading to a reaction product with sufficiently long half-life is ^{30}Si. The relevance of the reaction ^{30}Si$(p,n)^{30}$P was verified by following the time dependence of the positron-emission-related 511 keV annihilation peak. From the point of view of the present study, the significant nuclear reaction data[7] are provided in Table II. Also several other reactions are possible for silicon and copper, but the half-lives of the reaction products are clearly shorter or irrelevantly long. In several cases, the reaction cross sections are also insignificantly low. An important fact is that both of the produced radionuclides, ^{30}Si and ^{63}Zn, are positron emitters and as the positrons lose energy inside the detector they generate electron-hole pairs, which contribute to the dark current of the reverse biased device. Our conclusions were further verified by performing tests with 6 MeV protons, for which the radionuclide production cross sections are evidently lower. At this energy no activation-induced effects, e.g., breakdown, were noted.

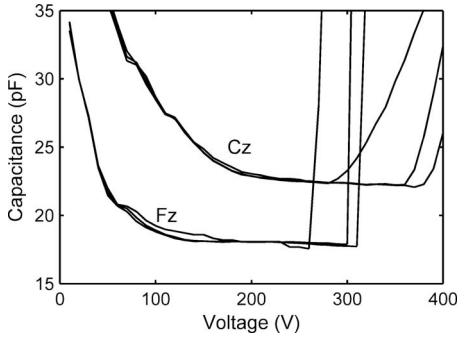

FIG. 4. *CV* curves for Fz and Cz detectors at various times after 5×10^{11} cm^{-2} irradiation with 9 MeV protons. The curves (from left to right) for the Fz detector correspond to measurements taken 10, 14, and 20 min after the irradiation and for the Cz detector 13, 19, and 25 min after the irradiation. The estimated full depletion voltages of the Fz and Cz detectors are about 120 and 195 V, respectively. The difference in the capacitance level between the detectors is due to their different physical dimensions. The detector temperature was kept at 250 K during the irradiations and measurements.

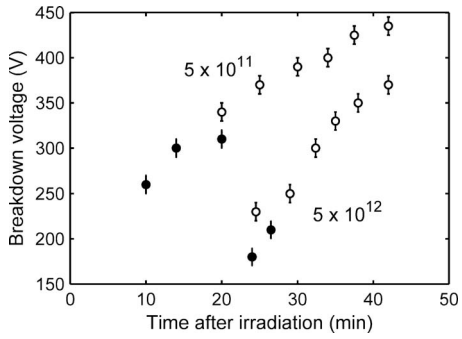

FIG. 5. Recovery of breakdown voltage of the Fz detector after 9 MeV proton irradiation to fluences of 5×10^{11} and 5×10^{12} cm^{-2} with a flux of $\sim4\times10^{10}$ protons/cm^2 s. The data have been extracted from *CV* curves of diodes irradiated and measured at 220 (open symbols) and 250 K (closed symbols).

IV. CALCULATIONS

To test the possibility that the proposed activation generated effects may result in the noted high leakage currents, the activation of the detector structure and the resulting leakage current were calculated by modeling the processes involved. Because stopping powers and reaction cross sections vary as a function of proton energy, the positron-emitting radionuclides are not produced uniformly within the detector structure (the actual detector structure with 300 μm Si thickness was utilized in the calculations). Proton stopping powers provided by the SRIM program,[8] reaction cross sections of Refs. 9 and 10, and the natural isotopic abundances of the elements involved were used.

The calculated distribution of ^{30}P nuclei produced by 7 MeV proton irradiation has a median value of 46 μm and it extends up to 153 μm from the detector surface (taking into account the recoil energy of the reaction product). Irradiation of the detector with 10^{14} protons/cm^2 yields approximately 1×10^9 ^{30}P nuclei produced within the silicon layer. In the case of 9 MeV protons the energy is sufficient to create ^{30}P nuclei within the whole 300 μm thick silicon layer and the median value of the distribution is 125 μm. Respectively, 10^{14} protons/cm^2 yield about 3×10^9 ^{30}P nuclei within the silicon layer. The 9 MeV protons lose 3 MeV in the Si layer and thus their energy is well above the 4.2 MeV threshold of the reaction ^{63}Cu$(p,n)^{63}$Zn. This enables positron production within the whole 30 μm thick copper layer since the proton energy decreases only to 4.8 MeV after penetration through the Cu layer [see Fig. 1(a)]. In the Cu layer 10^{14} protons/cm^2 yield approximately 5×10^9 ^{63}Zn nuclei.

The positrons, with defined energy distribution,[11] will be emitted to all directions and naturally only those positrons

TABLE II. Relevant proton-induced nuclear reactions leading to β^+-emitters (Ref. 7).

			Ground state β^+-decay	
Reaction	Threshold (keV)	Half-life (min)	End-point energy (keV)	Branching ratio (%)
^{30}Si$(p,n)^{30}$P	5183	2.5	3210	99.9
^{63}Cu$(p,n)^{63}$Zn	4215	38.5	2345	92.7

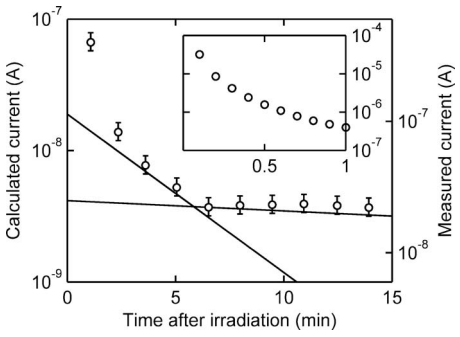

FIG. 6. Calculated currents induced during slowing down of positrons that are emitted by the ^{30}P and ^{63}Zn nuclei produced via 9 MeV proton irradiation (solid lines). The calculations are based on the actual Cz-detector layout presented in Fig. 1 and on the fluence and other parameters of Fig. 2. For comparison, the measured currents for a detector biased at 400 V are presented by the open symbols; note the different scales. The error bars represent the effect of possible temperature variation during the measurements (Ref. 14). The inset describes the effect of the short-lived positron-emitting reaction products. In the insert the error bars are within the symbol size.

that lose energy within the Si layer can generate *e-h* current. Monte Carlo simulations of the energy loss of the positrons inside the detector have been carried out taking into account the depth distributions of the positron emitters and the corresponding positron energy distributions. In the calculations, the electron stopping powers of the ESTAR code[12] have been used, taking into account the minor difference in the stopping powers of electrons and positrons.[13] In the case of 7 MeV protons, the average energy loss in silicon of a positron emitted in the decay of ^{30}P is 140 keV, and in the case of 9 MeV protons, it is 145 keV. The average energy loss in silicon of a positron emitted in the decay of ^{63}Zn, produced via 9 MeV proton irradiation, is 109 keV. Assuming that all of the energy deposited by the positrons inside the Si layer leads to *e-h*–pair creation (the value of 3.62 eV has been used for *e-h*–pair creation energy in Si), the consequent generated currents were calculated. Taking also into account the decay of the radioisotopes, the time behavior of the generated currents was depicted. The result for the Cz-detector structure irradiated with 9 MeV protons employing the fluence and other parameters of Fig. 2 is shown in Fig. 6. For comparison, the measured currents for a detector biased at 400 V are also presented. As the full depletion voltages were not measured, the value of 400 V was selected to ensure good charge collection efficiency. The estimated full depletion voltage is about 250 V employing a hardness factor of 5 for 9 MeV protons.[15] As may be noted, the calculations reproduce well the shape of the experimental time dependence. Both the experimental points and calculations expose clearly the components corresponding to decay of ^{30}P and ^{63}Zn, but the calculated currents are lower by a factor of 6. This difference may be attributed to the uncertainties in the input parameters used in the simulations, to the overestimation of the full depletion voltage, and to possible physical processes not modeled (e.g., thermal bulk current). For comparison, the thermally stimulated bulk current at 400 V for a detector irradiated with 7 MeV (hardness factor 7.3) protons saturates to the value of 12 nA (Fig. 3). The prominent effect of the short-lived positron-emitting reaction products on the measured currents is shown in the insert.

It should be noted that annihilation of thermalized positrons with electrons is the most probable annihilation process but its effect on the generated currents is negligible. In the annihilation-in-flight process, the kinetic energy of the positron is transferred to the γ-quanta and is not anymore available for *e-h*–pair creation. However, the probability for annihilation in flight is only a few percent.[16] Thus, in the present calculations, positron annihilation effects were not taken into account.

V. DISCUSSION AND CONCLUDING REMARKS

According to Figs. 2 and 3 the *IV* curves stabilize in about 5 and 10 min after 7 and 9 MeV proton irradiations, respectively. Because of the longer half-life of ^{63}Zn, the activation of the copper electrode is a function of the irradiation time and its effect is more prominent in the *CV* measurements. When irradiations longer than a few ^{30}P half-lives are performed, the activity of silicon depends rather on the irradiation flux than on the fluence since most ^{30}P nuclei decay already during the irradiation process. From Fig. 4 it may be noted that the activation of the copper electrode does not contribute to the *CV*-curve shape at voltages below 250 V. It should be noted that determination of the full depletion voltage from the Cz-detector *CV* data, which are measured first, is difficult if the commonly accepted method is used by plotting the data in a C^{-2} versus V graph and finding the intersection of the two fitted lines. Reasonable *IV* and *CV* curves can be expected only after some time.

According to the measured *CV* curves, the detectors are fully depleted prior to the appearance of the activation effect and subsequently the depletion region starts to break at a specific breakdown voltage. In the case of Fz detectors, the breakdown is abrupt and the high voltage values (Fig. 5) indicate typical avalanche multiplication.[17] The *e-h* current generated by the energetic positrons seems to amplify the multiplication considerably although the fluence of 5×10^{11} cm^{-2} is more than two orders of magnitude lower than the one used in the calculations of Fig. 6 and accordingly should lead to low current values. The effect of positrons on the breakdown voltage is surprisingly strong. It should be noted that the calculated currents correspond to an average value, but the actual peak currents can be higher. The recovery of the breakdown voltage is clearly affected by the irradiation fluence, which in turn affects the activity of ^{63}Zn, but the recovery is not affected by the detector temperature.

The suggested mechanism for the breakdown is as follows. Building up of oxide charge[18] leads to increased electric field strength near to the border of the *p-n*-junction and the oxide-silicon interface. Since in the oxide the mobility of holes is rather low and of electrons high, the holes induced by the positrons charge the oxide positively and this may then trigger localized charge carrier multiplication leading to the avalanche breakdown. This hypothesis would have to be substantiated by further experiments.

In summary, proton irradiation of Cz and Fz grown sili-

con particle detectors and the effect of material activation on their current-voltage and capacitance-voltage characteristics have been studied. The positron-generated *electron-hole* current affects drastically both *IV* and *CV* measurements by increasing the leakage current level and lowering the breakdown voltage. In the case of on-line electrical characterization of silicon particle detectors, it is compulsory that about 15 min is waited after the irradiation before starting the measurements. Clearly all materials that may become activated and lead to positron emitters with relevant half-life should be avoided in the detector concept.

ACKNOWLEDGMENT

The financial support from the Academy of Finland (Project No. 119260) is gratefully acknowledged.

[1]N. Meidinger, B. Schmalhofer, and L. Strüder, IEEE Trans. Nucl. Sci. **45**, 2849 (1998).
[2]N. Meidinger, B. Schmalhofer, and L. Strüder, Nucl. Instrum. Methods Phys. Res. A **439**, 319 (2000).
[3]D. Bechevet, M. Glaser, A. Houdayer, C. Lebel, C. Leroy, M. Moll, and P. Roy, Nucl. Instrum. Methods Phys. Res. A **479**, 487 (2002).
[4]G. Lindström, Nucl. Instrum. Methods Phys. Res. A **512**, 30 (2003).
[5]S. Väyrynen, P. Pusa, P. Sane, P. Tikkanen, J. Räisänen, K. Kuitunen, F. Tuomisto, J. Härkönen, I. Kassamakov, E. Tuominen, and E. Tuovinen, Nucl. Instrum. Methods Phys. Res. A **572**, 978 (2007).
[6]V. Kažukauskas, R. Jasiulionis, V. Kalendra, and J.-V. Vaitkus, Diamond Relat. Mater. **16**, 1058 (2007).
[7]http://www.nndc.bnl.gov/.
[8]http://www.srim.org/.
[9]S. Tanaka, N. Yamano, and K. Hata, Proceedings of the Eighth International Conference on Radiation Shielding, 1994 (unpublished), ANS Vol. 2, p. 965.
[10]S. Tanaka, M. Fukuda, K. Nishimura, H. Watanabe, and N. Yamano, "IRACM: A code system to calculate induced radioactivity produced by ions and neutrons," JAERI-Data/Code No. 97-019 (1997).
[11]http://nucleardata.nuclear.lu.se/nucleardata/toi/.
[12]http://physics.nist.gov/PhysRefData/Star/Text/ESTAR.html/.
[13]F. Rohrlich and B. C. Carlson, Phys. Rev. **93**, 38 (1954).
[14]F. Lehner, DØ note 3959, draft 2.0 (2002).
[15]E. Tuovinen, J. Härkönen, P. Luukka, E. Tuominen, E. Verbitskaya, V. Eremin, I. Ilyashenko, A. Pirojenko, I. Riihimäki, A. Virtanen, and K. Leinonen, Nucl. Instrum. Methods Phys. Res. A **568**, 83 (2006).
[16]G. Azuelos and J. E. Kitching, At. Data Nucl. Data Tables **17**, 103 (1976).
[17]S. M. Sze, *Semiconductor Devices* (Wiley, New York, 1985).
[18]G. Lutz, *Semiconductor Particle Detectors* (Springer-Verlag, Berlin, 1999).